PLOS WATER

RESEARCH ARTICLE

Worldwide moderate-resolution mapping of lake surface chl-a reveals variable responses to global change (1997–2020)

Benjamin M. Kraemer[1]*, Karan Kakouei[1], Catalina Munteanu[2], Michael W. Thayne[1,3,4], Rita Adrian[1,3]

1 IGB Leibniz Institute for Freshwater Ecology and Inland Fisheries, Berlin, Germany, **2** Albert-Ludwigs-University of Freiburg, Freiburg, Germany, **3** Freie Universität of Berlin, Berlin, Germany, **4** University of Geneva, Geneva, Switzerland

* ben.m.kraemer@gmail.com

Citation: Kraemer BM, Kakouei K, Munteanu C, Thayne MW, Adrian R (2022) Worldwide moderate-resolution mapping of lake surface chl-a reveals variable responses to global change (1997–2020). PLOS Water 1(10): e0000051. https://doi.org/10.1371/journal.pwat.0000051

Editor: M. J. M. Cheema, PMAS Arid Agriculture University: University of Arid Agriculture, PAKISTAN

Received: March 3, 2022

Accepted: September 22, 2022

Published: October 18, 2022

Data Availability Statement: GlobColour data (http://globcolour.info) used in this study has been developed, validated, and distributed by ACRI-ST, France. Geospatial and morphometric data for each lake is available from the previously published HydroLAKES database under the identifier doi: 10.1038/ncomms13603 and can be found at http://www.hydrosheds.org. All code used here are available under the identifier, DOI: 10.5281/zenodo.5026693.

Abstract

Anthropogenic activity is leading to widespread changes in lake water quality—a key contributor to socio-ecological health. But, the anthropogenic forces affecting lake water quality (climate change, land use change, and invasive species) are unevenly distributed across lakes, across the seasonal cycle, and across space within lakes, potentially leading to highly variable water quality responses that are poorly documented at the global scale. Here, we used 742 million chlorophyll-a (chl-a) estimates merged over 6 satellite sensors (daily, 1 to 4 km resolution) to quantify water quality changes from 1997 to 2020 in 344 globally-distributed large lakes. Chl-a decreased across 56% of the cumulative total lake area, challenging the putative widespread increase in chl-a that is expected due to human activity. 19% of lakes exhibited both positive and negative chl-a trends (p-value < 0.1) across different locations or times of the year. This spatiotemporal complexity demonstrates the value of moderate resolution mapping of lake chl-a to inform water management decision-making and to determine the local ecological consequences of human activity.

Introduction

Nutrient pollution and climate change may increase lake chlorophyll-a (chl-a) concentrations through various direct and indirect pathways [1, 2]. For instance, industry, agriculture, and urbanization have caused well-documented increases in chl-a by delivering nutrients to lakes through runoff and atmospheric deposition [1]. In addition, climate change can increase chl-a through the temperature dependence of primary production [3], by expanding the stratified season [4], or by promoting lake conditions which favor bloom-forming algae [5–8]. Land use and climate change can interact leading to synergistic increases in chl-a concentrations [9] with potential negative consequences for the millions of people who depend on lakes for their livelihoods [10].

However, global change is also associated with decreases in lake chl-a in some contexts. Climate change has been shown to reduce chl-a by impeding the entrainment of deep water

Funding: BMK, KK, and RA received funding from the 2017-2018 Belmont Forum and BiodivERsA joint call for research proposals under the BiodivScen ERA-Net COFUND programme with funding from the German Science Foundation (Deutsche Forschungsgemeinschaft; AD 91/22-1). MWT and RA received funding from the H2020 Marie Skłodowska-Curie Actions (722518) under the EU-ITN MANTEL project. CM acknowledges support from the German Science Foundation (Deutsche Forschungsgemeinschaft) Research Training Group ConFoBi (GRK 2123/1 TPX). The funders had no role in study design, data collection and analysis, decision to publish, or preparation of the manuscript.

Competing interests: The authors have declared that no competing interests exist.

nutrients into the surface waters where it is available to support algae growth [11–13] particularly in nutrient-poor lakes [14, 15]. Increased temperatures may also reduce chl-a when temperature-induced increases in the consumption and degradation of algae outpace temperature-induced increases in algal production [16, 17]. Neobiota can affect chl-a indirectly through trophic cascades or directly by grazing. For instance, neobiotic filter feeding mussels reduce chl-a by rapidly filtering lake water [18, 19]. Localized reductions in aquatic nutrient pollution can also reduce chl-a [20–22]. Climate or land use driven changes in water clarity can also influence chl-a and it's detection from space [23].

These environmental changes are unevenly distributed across lakes, across the seasonal cycle, and across space within lakes, potentially leading to highly heterogeneous water quality responses [1]. But this heterogeneity is not yet well-captured at the global scale. Thus, it remains uncertain whether the environmental changes operating a global scale tend to increase or decrease chl-a. An understanding of global patterns and spatial heterogeneity in long-term changes in lake water quality at sufficient spatiotemporal resolution is necessary for improving our macroecological understanding of lake ecosystems in a rapidly changing world. This improved understanding would also allow managers to design and implement more precisely targeted restoration strategies that are ultimately more effective at safeguarding lake resources [24].

Past global syntheses of long-term trends in chl-a at the global scale have treated lakes as discrete units with homogenous spatiotemporal changes [2, 15]. Here, we use a less discretized approach [25] focusing on within-lake changes at the daily temporal scale and at moderate spatial resolution (1km spatial resolution for Europe and 4 km spatial resolution for the rest of the world). We used 742 million chl-a estimates merged across 6 satellite sensors (SeaWiFS, MODIS AQUA, MERIS, OLCI-B, VIIRS NPP, and VIIRS JPSS-1) to assess long-term trends in 344 large lakes (surface area greater than 100 km^2) under ice-free and cloud-free conditions from 1997 to 2020. The 344 lakes included in our study represent 94% of Earth's liquid surface water by volume and contain a global heritage of freshwater biodiversity and natural resources. To detect chl-a, we used algorithms developed for coastal and inland waters [26] which we calibrated for specific lakes according to their mean depth, surface area, and shoreline complexity using Boosted Regression Trees (BRTs). This lake-specific algorithm calibration was based on comparing remote sensing and *in situ* chl-a data in 56 lakes where a total of 20,165 *in situ* chl-a estimates were available. We estimated the uncertainty in chl-a trends using bootstrapped error propagation techniques [27] incorporating the uncertainty in the chl-a algorithm and the lake-specific algorithm calibration.

Method

Overview

We calculated long-term (1997–2020) chl-a trends using 23 years of remote sensing data for 344 lakes (listed in S1 Table). Trends were calculated from chl-a anomalies where the effects of the day of the year, latitude, longitude, and remote sensing platform as well as the interactions between these variables had been accounted for and removed from the data. We calculated a single lake-wide trend where chl-a anomalies were pooled across pixels and seasons for each lake. We also calculated separate trends for each pixel (where chl-a anomalies were pooled across all days of the year) and for each day of the year (where chl-a anomalies were pooled across pixels). The size of the pixels was 1-km for lakes in Europe and 4-km for the rest of the globe based on the limitation of the data source used here [28].

Remote sensing chl-a data

We used 742 million chl-a estimates merged across 6 space-borne spectroradiometers (SeaWiFS, MODIS AQUA, MERIS, OLCI-B, VIIRS NPP, and VIIRS JPSS-1) to assess long-term trends in 344 lakes under ice-free and cloud-free conditions from year 1997 to 2020. Chl-a data were retrieved from the "CHL-OC5" product produced by GlobColour [28] and made available via the Copernicus Marine Environmental Monitoring Service (CMEMS) website: http://marine.copernicuseu/services-portfolio/access-to-products/. Only the highest-quality chl-a values were used according to the quality criteria provided as part of the CHL-OC5 data product resulting the exclusion of 76% of data due to partial cloud or ice cover. The algorithm used in the CHL-OC5 data product is a five-channel chlorophyll concentration algorithm which was developed for optically complex "case II waters" [26] and has been partially validated using global *in situ* data from marine and inland waters [29–31]. We built on this validation by expanding it to *in situ* data from 53 lakes as described below. The daily chl-a data reflect lake environments in the near surface layer during ice-free and cloud-free conditions. The seasonal extent and the number of chl-a estimates varied across lakes ranging from 2601 estimates for Lake Mogotoyeyo to 365 million for Lake Ladoga. We downloaded and processed the chl-a values in the R environment for statistical computing [32] using the "data.table" [33], "dismo" [34], "sf" [35], "gbm" [36], "zyp" [37] and "lubridate" [38] packages. Data visualizations were made using "ggplot2" [39].

Chl-a algorithm cross validation and calibration for inland waters

We adapted remotely sensed chl-a values specifically for lakes based on a comparison of 20,165 *in situ* chl-a measurements (chl-a extracted from filtered water samples) from 56 lakes matched to interpolated remote sensing data. To interpolate the remote sensing chl-a values, we used fully deterministic BRTs (bag fraction = 1) which modelled remotely sensed chl-a as a function of the decimal date, day of the year, sensor, latitude, and longitude separately for each lake. We used the resulting boosted regression trees (BRTs) to estimate remotely-sensed chl-a concentrations for all 6 sensors at the time and location of each *in situ* measurement. These modeled values served as the remotely-sensed matchup value for each *in situ* measurement. *In situ* data used for this purpose were downloaded, digitized, and compiled from published sources (S2 Table; mean chl-a = 8.7 μg L^{-1}, median chl-a = 3.9 μg L^{-1}, range = 0.01 to 579.2 μg L^{-1}). We would expect the calibrated chl-a algorithm used here to be less accurate near the tails and outside of the *in situ* chl-a distribution.

We modelled the difference between *in situ* values and their remotely sensed matchup values as a function of the raw remotely sensed chl-a value, the *in situ* data source, and 3 lake characteristics (mean lake depth, surface area, and shoreline development index (a metric of shoreline complexity; the ratio of a lake's shoreline length to the circumference of a circle with the equivalent lake area)) also using a BRT. These three lake characteristic variables were used because they are associated with lake optical characteristics [40] and are freely available from the HydroLAKES database [41]. Thus, the BRT allowed the difference between *in situ* and remotely sensed chl-a values to vary from lake to lake. We then used the resulting model to estimate the difference between *in situ* and remotely sensed values for all 742 million chl-a estimates used here. We translated the remotely sensed chl-a values into an "*in situ* analogue" chl-a value by subtracting the modelled differences from the raw remotely sensed values. The resulting *in situ* analogue chl-a values were used for all subsequent analyses. The calibration of the algorithm using *in situ* chl-a data reduced the median absolute error from 3.6 μg L^{-1} to 1.5 μg L^{-1}.

Chl-a anomaly calculations

To estimate lake surface chl-a anomalies, we accounted for and removed variation in each lake's *in situ* analogue chl-a data which could be attributed to the day of the year, latitude, longitude, and sensor using BRTs. Thus, the chl-a anomalies were defined as the residuals from a BRT predicting *in situ* analog chl-a as a function of four predictor variables—the day of the year, latitude, longitude, and sensor. This approach allowed us to account for patchiness in the chl-a data [42] and bypass the need for gap-filling the time series. This allowed for the calculation of trends over time in chl-a anomalies such that the trends would be less influenced by the seasonal or spatial coverage of the data, the sensor timespan or the interactions among these factors. For the BRTs, we used a tree complexity of 5 to allow for high levels of interactions among variables (e.g. sensor type could have different effects on *in situ* analog chl-a at specific grid cells within lakes and at specific times of the year). To prevent model overfitting, the BRTs were fit separately for each lake 10 times using a randomly selected 50% of the data. Predicted values were generated from each of the 10 models for all chl-a estimates and averaged to generate more robust estimates. The residuals (i.e. difference between the *in situ* analog chl-a values and the average of the 10 model predictions) were termed, "chl-a anomalies." We confirmed that this process successfully removed the variation attributable to the day of the year, latitude, longitude, and sensor using visual diagnostic plotting for all lakes (see example for Lake Erie in S6 Fig).

BRTs include a variety of tuning parameters which influence the model performance in cross validation. We selected a combination of tuning parameters (bag fraction = 0.62, tree complexity = 5) which reliably gave good performance in 10-fold cross validation across all lakes (median predicted residual error sum of squares = 0.35 μg L^{-1}, and median correlation between predicted and observed values = 0.85). We optimized the learning rate separately for each of the 10 BRTs for each lake by iteratively running the model with smaller and smaller learning rates (from 0.8, 0.4, 0.2, 0.1, 0.05, to 0.025) until the number of trees in the BRT which minimized the predicted deviance was greater than 1000 as suggested in previous literature [43].

Chl-a trends

We used a bootstrapped error propagation technique [27] to estimate chl-a trends and the uncertainty in each trend. The residual errors from the BRT used for adapting remotely sensed chl-a into *in situ* analogue values were propagated into the estimate of chl-a trend uncertainty. We propagated the errors by adding a residual error (the product of a randomly selected % error residual from the BRT's error distribution and the original *in situ* analogue chl-a value) to each chl-a anomaly. Distinct residual errors were iteratively added to each chl-a anomaly value with 100 repetitions. For each repetition, Theil-Sen slopes and intercepts were calculated based on mean annual chl-a anomalies. We calculated p-values of a Spearman rank correlation test relating mean chl-a anomalies to year. The trends and their associated p-values were calculated as the average across all 100 repetitions of the Theil-Sen slope and Spearman correlation calculations.

We calculated a single lake-wide trend where chl-a anomalies were pooled across pixels and seasons for each lake. We also calculated separate trends for each pixel (where chl-a anomalies were pooled across all days of the year) and for each day of the year (where chl-a anomalies were pooled across pixels). Chl-a percent change was calculated from Theil-Sen nonparametric regression in chl-a anomalies after the effects of the day of the year, latitude, longitude, and sensor as well as the interactions between these variables had been accounted for and removed from the data. Theil-Sen nonparametric regression results were translated into a proportion

change by taking the difference between the Theil-Sen modelled chl-a anomalies in 2020 and 1997 as a proportion of the lake's median chl-a *in situ* analog value. This proportion was translated into a percentage by multiplying by 100. All stationary variation in chl-a due to space and season was removed using machine learning (BRT) prior to the calculation of trends, thus we would not expect strong bias in the chl-a trends related to ice/cloud cover.

Results and discussion

We found that when chl-a trends were calculated as lake-wide averages, the median chl-a trend across all lakes was +0.04 μg chl-a decade^{-1} (total range = -11.98 to +9.64 μg chl-a decade^{-1}, interquartile range = -0.03 to 0.27 μg chl-a decade^{-1}, median % change = +3.2; Fig 1A). Lake-wide average chl-a increased in 65% of lakes (225 out of 344; Fig 2) and decreased in the remaining 35%. Increasing trends in 142 lakes and decreasing trends in 68 lakes had p-values less than 0.1. Thus, more lakes had trends with p-values less than 0.1 than what would be expected based on chance alone and this was true regardless of which arbitrary threshold was used (we tested p-value cutoffs of $\alpha = 0.1, 0.05, 0.01$). These general findings are comparable to previous work based on Landsat imagery which found that 68% of large lakes had increasing chl-a concentrations since the 1980's and 39% of lakes had trends with p-values less than 0.1 [2].

The lake-wide average trends agreed well with published literature on phytoplankton, chl-a, and other phytoplankton proxies based on *in situ* data sources. For example, *in situ* phytoplankton biomass proxies decreased in Lake Tanganyika as enhanced thermal stratification due to climate change has reduced the entrainment of deep-water nutrients and primary production [11, 12, 44] (Fig 1). Conversely, chl-a variation in Lake Kivu shown here (Fig 1) matched a strong cycle in phytoplankton biomass observed *in situ* due to background climate variation [45]. Remotely-sensed chl-a also increased in Lake Erie which has experienced a well-documented nutrient pollution trend for decades due to agricultural expansion and intensification [46] (Fig 1).

While 63% of lakes had positive chl-a trends at the lake-wide average scale, only 44% of the total lake area experienced increases in chl-a at the pixel scale. This difference arose because chl-a tended to decrease in the largest lakes (Fig 1A). The global median chl-a trend was -0.01 μg chl-a decade^{-1} when pixel-level trends were weighted by pixel area (pixel area varies across latitude when a consistent equal angle grid is applied). In total, we investigated chl-a trends at the pixel scale for 1,383,893 km^2 of cumulative lake area. Chl-a increased for 612,014 km^2 of the cumulative lake area and 17% (104,871 km^2) had a p-value less than 0.1. Chl-a decreased across 771,879 km^2 of the cumulative lake area and 19% (148,175 km^2) of the lake area with decreasing trends had p-values less than 0.1. Thus, more lake area had trends at the pixel scale with p-values less than 0.1 than what would be expected based on chance alone which was also true using a cutoff of 0.05, and 0.01. This finding (Fig 2D) challenges the broadly held assumption that global change has caused widespread increases in lake chl-a [1].

Decreases in chl-a observed here have been attributed to water management efforts in some lakes (e.g. Ladoga [47]), and to invasive filter feeding mussels in others (e.g. Ontario, Huron, Michigan [21]), but these drivers alone cannot explain decreases across all lakes. Decreases in chl-a as a result of climate change through changes to terrestrial inputs [48], higher heterotrophic consumption of algae [49, 50], or climate change mediated reductions in deep water nutrient entrainment to the well-lit surface waters [4, 51–53] may be an underrecognized response to global change. While this result is most relevant for Earth's large lakes, widespread bluing trends have been observed in small lakes as well [48, 54, 55]. We recommend future emphasis on how global-change may reduce chl-a, especially because chl-a reductions can heavily affect lake ecosystems and the benefits that humans derive from them [20–22].

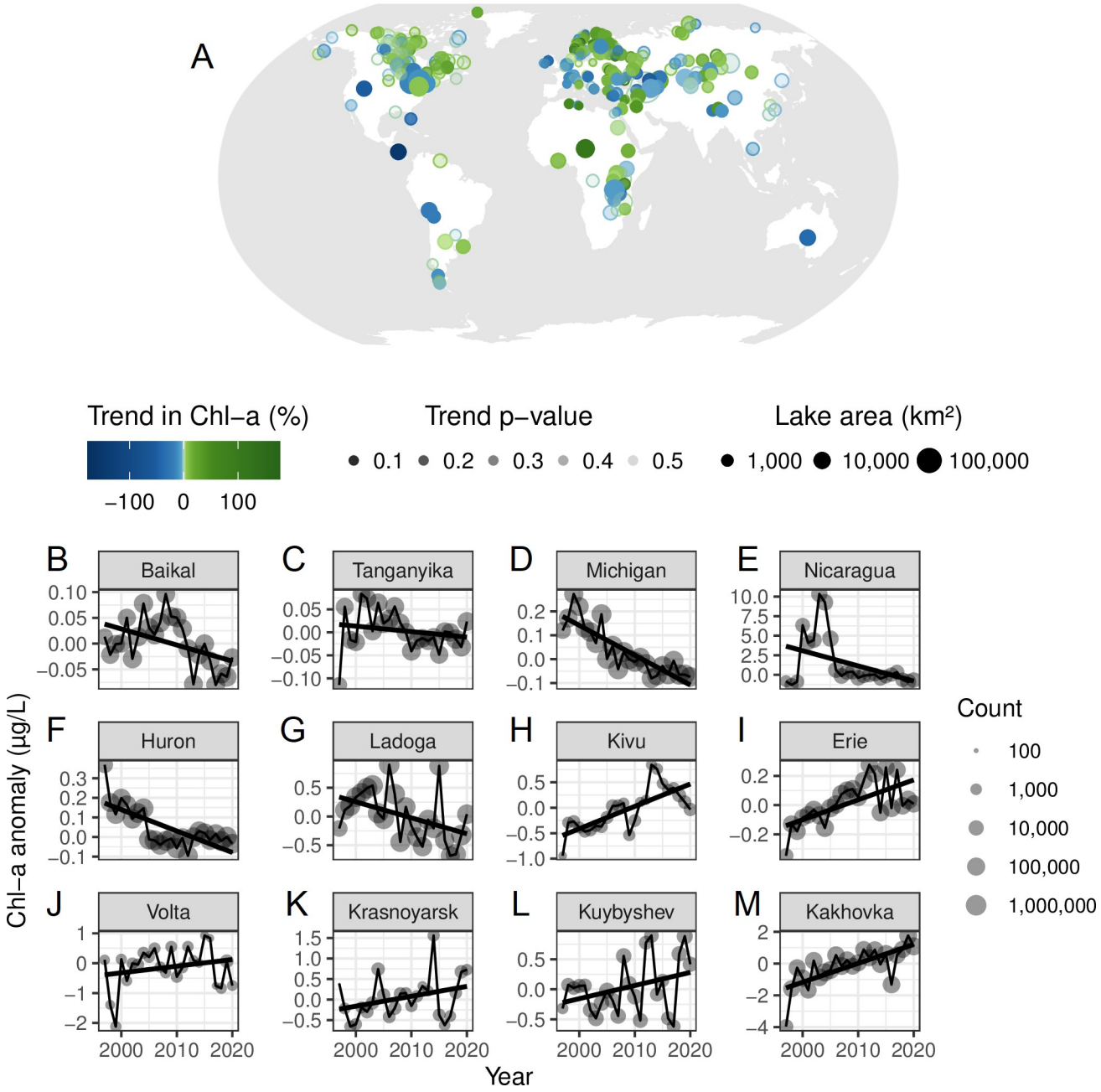

Fig 1. Chl-a percent change (1997–2020) based on lake-wide averages. Map showing lake-wide trends for 344 globally distributed lakes where the sizes of the dots are proportional to the size of the lake and the transparency of the dot is proportional to the p-value (**A**). Time series show the chl-a anomalies for the 6 lakes with the largest negative trends (**B:G**) in lake-wide chl-a and the 6 lakes with the largest positive trends (**H:M**) in lake-wide chl-a when trends were weighted by each lake's volume. The black lines (**B:M**) are the ordinary least squares regression line and the size of the dots represents the number of chl-a estimates in each year (**B:M**). An inset map of Europe can be found in S1 Fig. Continent boundary map data come from Natural Earth. (http://www.naturalearthdata.com/about/terms-of-use/; public domain).

https://doi.org/10.1371/journal.pwat.0000051.g001

Long-term trends based on lake-wide averages hid the complexity of long-term change in chl-a across lake surfaces. Some lakes which had weak overall chl-a trends at the lake-wide scale, had strong simultaneous increases and decreases in chl-a at different locations within the lake (Fig 3). For example, the Caspian Sea had a weak overall trend at the lake-wide scale but chl-a increased substantially in the northern shallows (Fig 3). Increasing trends in the

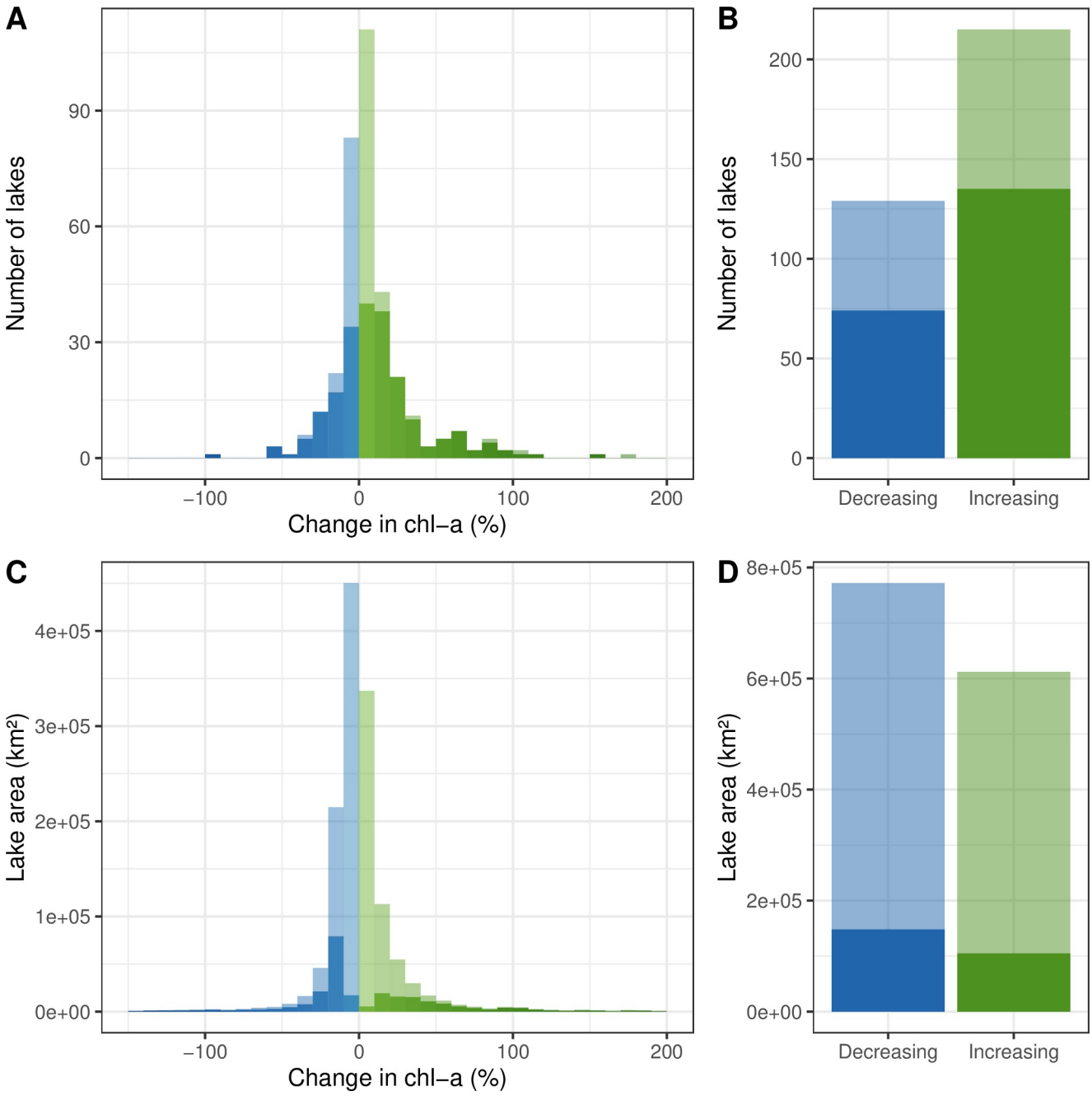

Fig 2. Distribution of global chl-a percent change (1997–2020). Percent change at the lake-wide average scale (**A**, **B**), and at the lake area scale based on pixel-level trends (**C**, **D**). Blue indicates decreasing trends and green indicates increasing trends. The solid portion of each bar represents the proportion of trends with p-values less than 0.1.

https://doi.org/10.1371/journal.pwat.0000051.g002

Caspian Sea primarily occurred near the inflowing Ural, Volga, and Terek rivers which deliver large nutrient loads from the surrounding landscape [56] (S2 Fig). At the lake-wide scale, this increase in chl-a in the northern shallows was offset by the statistically weaker but widespread decrease in chl-a in the deeper offshore areas (Fig 3).

In addition to the Caspian Sea, many other lakes experienced local increases in chl-a in the shallower areas closer to the shore near inflowing rivers that diverged from lake-wide average

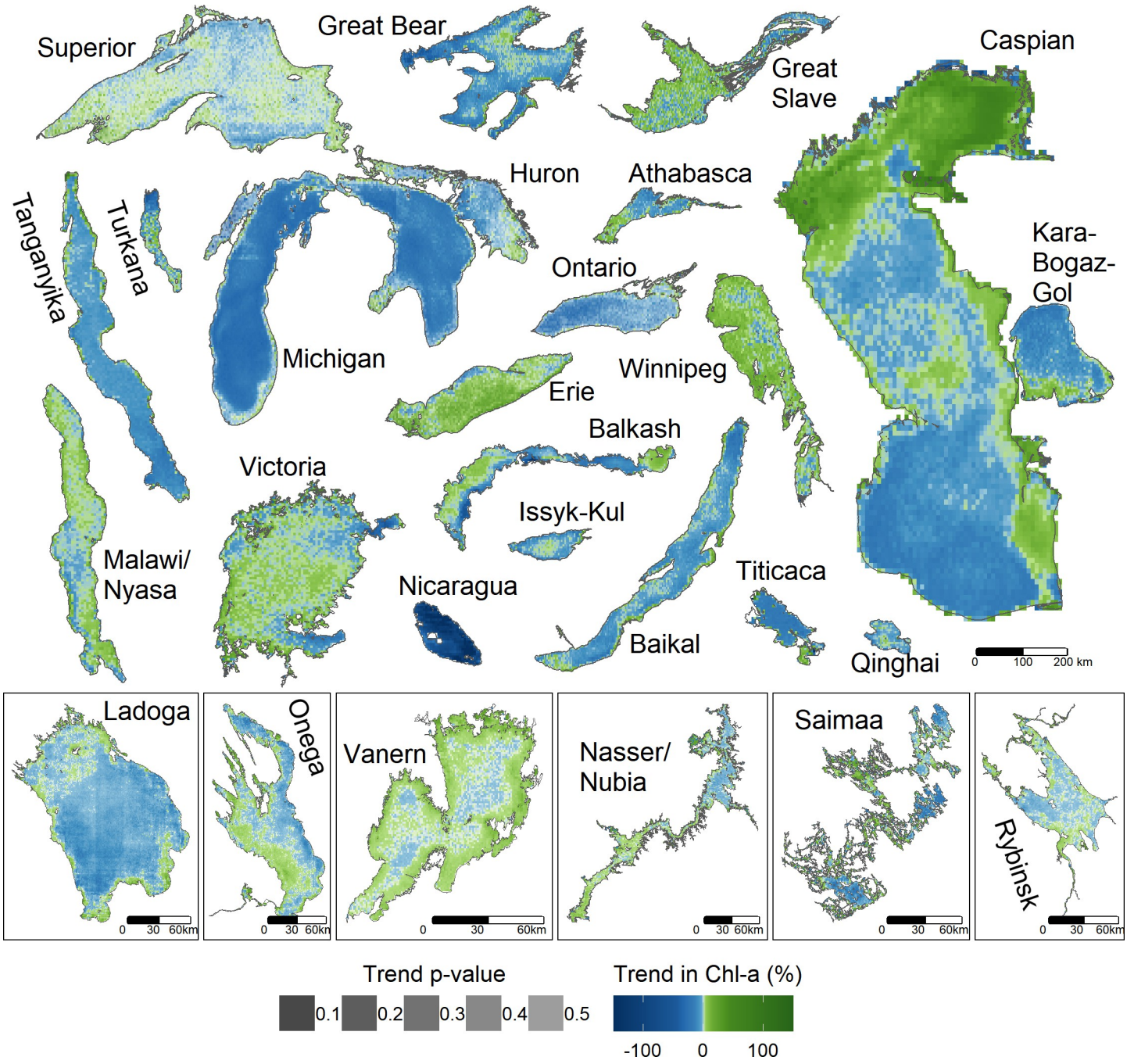

Fig 3. Spatial variation within and across lakes in chl-a trends (1997–2020). The relative positions of the lakes shown here do not reflect geo-spatial location but lake sizes share a common scale except where indicated otherwise in the boxed insets. Lakes shown are those with the largest number of chl-a estimates. The opacity of the color scale reflects the p-values associated with each pixel-level trend. The p-values associated with each grid cell can be found in S3 Fig. Lake boundary map data come from the HydroLAKES database v1.0 which is licensed under a Creative Commons Attribution (CC-BY) 4.0 International License. (https://www.hydrosheds.org/products/hydrolakes).

https://doi.org/10.1371/journal.pwat.0000051.g003

trends (Fig 3). For example, Lake Huron experienced very localized increases in chl-a in the shallow Saginaw Bay where the Saginaw River enters the lake bringing with it a variety of agricultural and industrial pollutants [57] (S2 Fig). At the same time, chl-a decreased in the

offshore deeper areas of Lake Huron where the combined effect of nutrient mitigation and invasive species expansion has caused reductions in chl-a [21]. Lake Titicaca experienced very localized increases in chl-a in the smaller south east basin where inflowing rivers drain an increasingly urbanized catchment near El Alto/La Paz, Bolivia [58] (S2 Fig). A strong reduction in chl-a concentrations in Lake Ladoga (Fig 3) suggests that continued efforts at reducing nutrient pollution have improved water quality there. However, patchy greening areas in the shallower parts of Lake Ladoga may indicate the potential for internal re-suspension of past phosphorus loads resting in the sediment [59]. Lake Nasser/Nubia, one of the largest manmade lakes in the world, has a pronounced greening trend near the inflowing Nile River which transitions into a bluing trend near the outflow of the reservoir. This transitioning from chl-a increases to decreases along the axis of water flow was common in large reservoirs presumably because nutrient loads from incoming rivers get diluted as they pass into larger volumes of water with greater thermal stratification. Thus, simultaneous increases and decreases in chl-a for specific locations within lakes can reflect differences in the location and strength of various anthropogenic stressors affecting chl-a. Chl-a changes at the local scale within lakes may diverge widely from the lake-wide average.

Long-term trends based on lake-wide averages also failed to capture the complexity of long-term change in lake surface chl-a across days of the year for individual lakes. For example, in Lakes Michigan, Huron, and Ontario, introduced mussels have reduced chl-a primarily in the less stratified times of the year when the impact of filter feeding on phytoplankton is strongest [19] (Fig 4). Chl-a decreases in Lake Tanganyika were most pronounced during the dry season when climate change mediated changes to stratification patterns have dampened seasonal mixing [11, 12]. Several lakes had serial increases and decreases in chl-a across the seasonal spectrum (Fig 4). For instance, earlier seasonal stratification in Lake Superior due to climate change may have increased chl-a in early spring when phytoplankton benefit from being

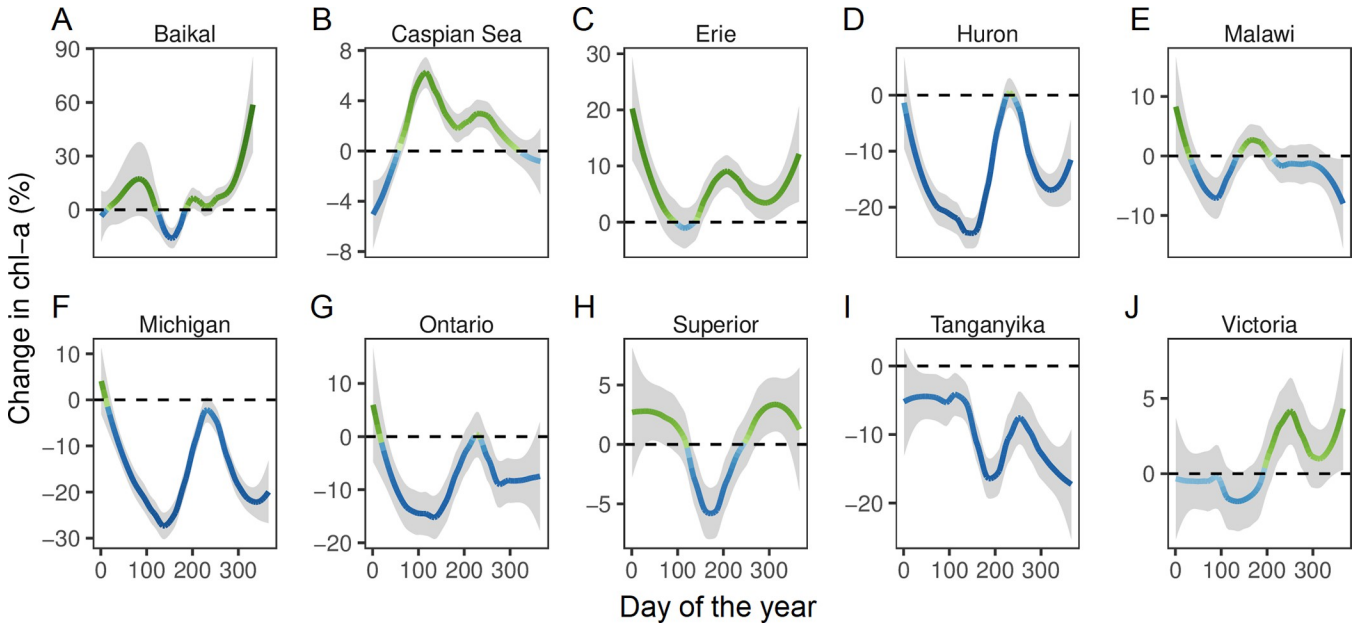

Fig 4. Seasonal variation in lake chl-a trends (1997–2020). Panels (**A:J**) show seasonal trends in chl-a for the 10 largest lakes with broad seasonal data coverage. Lines represent the LOESS-smoothed (span of 1) daily trend in chl-a weighted by the number of chl-a estimates included in the chl-a trend calculation for each day of the year. The blue to green color reinforces values on the y-axes and is consistent across panels. The shaded area represents the 95% confidence interval for the smoothed line.

https://doi.org/10.1371/journal.pwat.0000051.g004

retained in the well-lit stratified surface layer where they can better photosynthesize. But the increased chl-a in early spring in Lake Superior is combined with a summer decrease in chl-a as prolonged summer stratification reduces the amount of nutrients available for primary producers [60].

This within lake complexity (Fig 3, S4 Fig) and seasonal complexity (Fig 4) of chl-a trends discounts the tendency in lake management to emphasize the dichotomous view that lakes are either undergoing increases or decreases in chl-a. 19% of lakes exhibited positive and negative trends in chl-a at different locations or at different times of the year (i.e. more than 10% of positive trends and more than 10% of the negative trends had p-values less than 0.1). The lakes with both positive and negative trends represented 63% of the lake area. This combination of positive and negative trends for individual lakes highlights the heterogeneity of lake responses to global change. Whole-lake chl-a trends can mask spatiotemporal trend variability leading to lakes with weak trends at the lake-wide scale but strongly contrasting increases and decreases in chl-a at finer seasonal and spatial resolution (e.g. Caspian Sea in Figs 3 and 4). Policy makers and lake managers should recognize the potential for local changes at specific times of the year to vary widely from lake-wide averages. Major water management policies such as the Water Framework Directive (EU) and the Clean Water Act (USA) have established management targets based on lake-wide and annual averages which fail to capture the spatiotemporal complexity shown here. Instead, management decisions or policies should be based on finer metrics (i.e. not lake-wide or annual averages) which more fully recognize spatiotemporal variation in water quality and water quality trends.

Overall, we provide a global view of trends in near surface chl-a over the past 23 years for large lakes. Our analysis of chl-a in lakes demonstrates the promise of spatially-explicit long-term satellite observations for tracking chl-a conditions and disentangling the multiple overlapping drivers of change. The approach used here augments the geographically and temporally limited *in situ* chl-a monitoring efforts where data is often not shared readily nor in near real time. This analysis applies a novel statistical approach to merge chl-a data from multiple sensors to produce a validated data set that documents global lake surface chl-a dynamics with new levels of spatial detail and accuracy. Global datasets documenting the aquatic concentration of chlorophyll-a (chl-a) with remote sensing can serve as a key indicator of lake responses to human activity but so far have been underused. The accuracy of remote sensing based chl-a estimates has been questioned at the local scale due to the presence of surface algae scums, submerged vegetation, sediment, and high concentrations of organic matter [61–63]. However, the cross validation and the performance of the lake-specific chl-a algorithm developed here (S5 Fig) suggests that our main conclusions are robust to such effects. Nonetheless, we caution against the overinterpretation of specific trend estimates reported here and suggest corroborating observed trends in chl-a with *in situ* measurements wherever possible. In the frequent absence of such *in situ* measurements, remote sensing data of this type may provide the best approximation of global scale trends yet available.

Conclusion

Our primary result that chl-a concentrations decreased for 56% of lake area when calculated at the pixel scale challenges the putative widespread increase in chl-a intensity that is expected due to human activity [1, 2, 64]. Furthermore, we highlight that lake chl-a trends vary substantially across the surface of lakes, and across seasons making lake-wide average trends or patterns extrapolated from small central extraction points potentially misleading. The findings reported here reinforce the need for water-resource management strategies that integrate the potential for both increases and decreases in chl-a due to global change. Spatially-explicit

water quality monitoring is essential for evaluating the success of investments in water management and for detecting new management challenges. Management approaches that currently treat lake-wide surface chl-a trends in a simplistic fashion should immediately benefit from the detailed maps of chl-a trends provided here. Resolving key challenges in water management requires spatially- and temporally-explicit approaches that engage policymakers and water managers at scales relevant to their decisions, including subnational administrative units, bays, and delimited stretches of lake shoreline. The data used herein hold promise for identifying the timing and magnitude of lake phytoplankton variations at daily scales allowing lake scientists and managers to concurrently capture human influences on surface water quality in near real time. The need to mobilize financial resources to support integrated approaches using these data is imperative, before additional drift from past ecological conditions becomes the new accepted norm for lakes.

Supporting information

S1 Fig. Chl-a percent change (1997–2020) based on lake-wide averages for European lakes with data at higher spatial resolution (1 km x 1 km). The color of the dot indicates the trend with green values corresponding to increases in chl-a and blue values corresponding to decreases in chl-a. The opacity of the trend is proportional to its p-value with more opaque circles indicating more statistically stronger trends. The size of the dot is proportional to the area of each lake. Continent boundary map data come from Natural Earth. (http://www.naturalearthdata.com/about/terms-of-use/; public domain).
(TIF)

S2 Fig. Greening near the mouths of major inflowing rivers. Maps shown for Saginaw Bay, Lake Huron (**A**), the Northern Caspian Sea (**B**), and Lake Titicaca (**C**). Lake boundary map data come from the HydroLAKES database v1.0 and river map data come from the HydroSHEDS database, both of which are licensed under a Creative Commons Attribution (CC-BY) 4.0 International License. (https://www.hydrosheds.org/).
(TIF)

S3 Fig. P-values associated with trends across space within lakes. Lakes shown are the same as those in Fig 3. Darker reds indicate relatively higher statistical strength. P-values less than 0.5 appear white. Lake boundary map data come from the HydroLAKES database v1.0 which is licensed under a Creative Commons Attribution (CC-BY) 4.0 International License. (https://www.hydrosheds.org/products/hydrolakes).
(TIF)

S4 Fig. The proportion of lake area which exhibited decreases (blue bars) versus increases (green bars) in chl-a for the largest 18 lakes in the world. The darker portion of each bar represents the proportion of lake area which had p-values less than 0.1. The Caspian Sea is plotted separately to facilitate visualization of the smaller lakes which are plotted on a separate x-axis scale.
(TIF)

S5 Fig. Cross validation of remotely sensed chl-a. Relationship between *in situ* chl-a and the nearest raw remote sensing chl-a value (**A**). Relationship between *in situ* chl-a and the *in situ* analogue chl-a values after adapting the chl-a algorithm for specific lakes according to their characteristics (**B**). The shaded area reflects the density of the chl-a estimates at each gridcell. The red dots are the lake-wide averages for each of the 56 lakes where *in situ* chl-a data were available.
(TIF)

S6 Fig. Calculation of chl-a anomalies from *in situ* analog chl-a values. We used boosted regression trees to remove the variation in chl-a (*in situ* analog values) attributable to the sensor (**A**, **B**), the day of the year (**C**, **D**), and the location (latitude and longitude) (**E**, **F**). Locally weighted scatterplot smoothing (LOWESS) lines are shown for raw chl-a values (**A, C, E**) and chl-a anomaly values (**B, D, F**) demonstrating that the variation attributable to three variables (sensor, day of the year, and location) and their interactions was successfully removed by this method. Lake boundary map data come from the HydroLAKES database v1.0 which is licensed under a Creative Commons Attribution (CC-BY) 4.0 International License. (https://www.hydrosheds.org/products/hydrolakes).
(TIF)

S1 Table. List of all large lakes included in the analysis including their characteristics.
(XLSX)

S2 Table. *In situ* chl-a data used for chl-a algorithm calibration.
(XLSX)

Acknowledgments

We acknowledge the time and effort required of several anonymous reviewers who provided constructive feedback on previous versions of this manuscript.

Author Contributions

Conceptualization: Benjamin M. Kraemer, Karan Kakouei, Catalina Munteanu, Michael W. Thayne, Rita Adrian.

Data curation: Benjamin M. Kraemer.

Formal analysis: Benjamin M. Kraemer.

Funding acquisition: Rita Adrian.

Investigation: Benjamin M. Kraemer.

Methodology: Benjamin M. Kraemer.

Project administration: Benjamin M. Kraemer.

Resources: Benjamin M. Kraemer.

Software: Benjamin M. Kraemer.

Validation: Benjamin M. Kraemer.

Visualization: Benjamin M. Kraemer.

Writing – original draft: Benjamin M. Kraemer.

Writing – review & editing: Benjamin M. Kraemer, Karan Kakouei, Catalina Munteanu, Michael W. Thayne, Rita Adrian.

References

1. Oliver SK, Collins SM, Soranno PA, Wagner T, Stanley EH, Jones JR, et al. Unexpected stasis in a changing world: Lake nutrient and chlorophyll trends since 1990. Glob Change Biol. 2017;23. https://doi.org/10.1111/gcb.13810 PMID: 28834575
2. Ho JC, Michalak AM, Pahlevan N. Widespread global increase in intense lake phytoplankton blooms since the 1980s. Nature. 2019; 574: 667–670. https://doi.org/10.1038/s41586-019-1648-7 PMID: 31610543

3. Yvon-Durocher G, Allen AP, Cellamare M, Dossena M, Gaston KJ, Leitao M, et al. Five Years of Experimental Warming Increases the Biodiversity and Productivity of Phytoplankton. PLoS Biol. 2015;13. https://doi.org/10.1371/journal.pbio.1002324 PMID: 26680314
4. Woolway RI, Merchant CJ. Worldwide alteration of lake mixing regimes in response to climate change. Nat Geosci. 2019; 12: 271–276. https://doi.org/10.1038/s41561-019-0322-x
5. Kosten S, Huszar VLM, Bécares E, Costa LS, van Donk E, Hansson LA, et al. Warmer climates boost cyanobacterial dominance in shallow lakes. Glob Change Biol. 2012; 18: 118–126. https://doi.org/10.1111/j.1365-2486.2011.02488.x
6. Wagner C, Adrian R. Cyanobacteria dominance: Quantifying the effects of climate change. Limnol Oceanogr. 2009; 54: 2460–2468. https://doi.org/10.4319/lo.2009.54.6_part_2.2460
7. Paerl HW, Paul VJ. Climate change: links to global expansion of harmful cyanobacteria. Water Res. 2012; 46: 1349–63. https://doi.org/10.1016/j.watres.2011.08.002 PMID: 21893330
8. Woolway RI, Kraemer BM, Zscheischler J, Albergel C. Compound hot temperature and high chlorophyll extreme events in global lakes. Environ Res Lett. 2021; 16: 124066. https://doi.org/10.1088/1748-9326/ac3d5a
9. Rigosi A, Carey C, Ibelings B. The interaction between climate warming and eutrophication to promote cyanobacteria is dependent on trophic state and varies among taxa. Limnol Oceanogr. 2014; 59: 99–114.
10. Dodds WK, Bouska WW, Eitzmann JL, Pilger TJ, Pitts KL, Riley AJ, et al. Eutrophication of U.S. Freshwaters: Analysis of Potential Economic Damages. Environ Sci Technol. 2009; 43: 12–19. https://doi.org/10.1021/es801217q PMID: 19209578
11. O'Reilly CM, Alin SR, Plisnier P-D, Cohen AS, McKee BA. Climate change decreases aquatic ecosystem productivity of Lake Tanganyika, Africa. Nature. 2003; 424: 766–8. https://doi.org/10.1038/nature01833 PMID: 12917682
12. Tierney JE, Mayes MT, Meyer N, Johnson C, Swarzenski PW, Cohen AS, et al. Late-twentieth-century warming in Lake Tanganyika unprecedented since AD 500. Nat Geosci. 2010; 3: 422–425. https://doi.org/10.1038/ngeo865
13. Behrenfeld MJ, O'Malley RT, Siegel DA, McClain CR, Sarmiento JL, Feldman GC, et al. Climate-driven trends in contemporary ocean productivity. Nature. 2006; 444: 752–755. https://doi.org/10.1038/nature05317 PMID: 17151666
14. Michelutti N, Wolfe AP, Cooke CA, Hobbs WO, Vuille M, Smol JP. Climate change forces new ecological states in tropical Andean lakes. PLoS ONE. 2015; 10: e0115338. https://doi.org/10.1371/journal.pone.0115338 PMID: 25647018
15. Kraemer BM, Mehner T, Adrian R. Reconciling the opposing effects of warming on phytoplankton biomass in 188 large lakes. Sci Rep. 2017;7. https://doi.org/10.1038/s41598-017-11167-3 PMID: 28883487
16. Yvon-Durocher G, Montoya JM, Trimmer M, Woodward G. Warming alters the size spectrum and shifts the distribution of biomass in freshwater ecosystems. Glob Change Biol. 2011; 17: 1681–1694. https://doi.org/10.1111/j.1365-2486.2010.02321.x
17. Kraemer BM, Chandra S, Dell AI, Dix M, Kuusisto E, Livingstone DM, et al. Global patterns in lake ecosystem responses to warming based on the temperature dependence of metabolism. Glob Change Biol. 2017; 23: 1881–1890. https://doi.org/10.1111/gcb.13459 PMID: 27591144
18. Vanderploeg HA, Nalepa TF, Jude DJ, Mills EL, Holeck KT, Liebig JR, et al. Dispersal and emerging ecological impacts of Ponto-Caspian species in the Laurentian Great Lakes. Canadian Journal of Fisheries and Aquatic Sciences. 2002. https://doi.org/10.1139/f02-087
19. Warner DM, Lesht BM. Relative importance of phosphorus, invasive mussels and climate for patterns in chlorophyll a and primary production in Lakes Michigan and Huron. Freshw Biol. 2015; 60: 1029–1043. https://doi.org/10.1111/fwb.12569
20. Jeppesen E, Søndergaard M, Jensen JP, Havens KE, Anneville O, Carvalho L, et al. Lake responses to reduced nutrient loading—An analysis of contemporary long-term data from 35 case studies. Freshw Biol. 2005; 50: 1747–1771. https://doi.org/10.1111/j.1365-2427.2005.01415.x
21. Evans MA, Fahnenstiel G, Scavia D. Incidental oligotrophication of North American Great Lakes. Environ Sci Technol. 2011; 45: 3297–3303. https://doi.org/10.1021/es103892w PMID: 21417221
22. Anderson NJ, Jeppesen E, Søndergaard M. Ecological effects of reduced nutrient loading (oligotrophication). An introduction. Freshwat Biol. 2005; 50: 1589–1593.
23. Declining greenness in Arctic-boreal lakes | PNAS. [cited 28 Apr 2021]. Available: https://www.pnas.org/content/118/15/e2021219118

24. Vörösmarty CJ, McIntyre PB, Gessner MO, Dudgeon D, Prusevich A, Green P, et al. Global threats to human water security and river biodiversity. Nature. 2010; 467: 555–561. https://doi.org/10.1038/nature09440 PMID: 20882010

25. Kraemer BM. Rethinking discretization to advance limnology amid the ongoing information explosion. Water Res. 2020; 178: 115801. https://doi.org/10.1016/j.watres.2020.115801 PMID: 32348931

26. Gohin F, Druon JN, Lampert L. A five channel chlorophyll concentration algorithm applied to Sea WiFS data processed by SeaDAS in coastal waters. Int J Remote Sens. 2002; 23: 1639–1661. https://doi.org/10.1080/01431160110071879

27. Blukacz EA, Sprules WG, Brunner J. Use of the bootstrap for error propagation in estimating zooplankton production. Ecology. 2005; 86: 2223–2231. https://doi.org/10.1890/04-0772

28. Maritorena S, d'Andon OHF, Mangin A, Siegel DA. Merged satellite ocean color data products using a bio-optical model: Characteristics, benefits and issues. Remote Sens Environ. 2010; 114: 1791–1804.

29. Gbagir A-MG, Colpaert A. Assessing the Trend of the Trophic State of Lake Ladoga Based on Multi-Year (1997–2019) CMEMS GlobColour-Merged CHL-OC5 Satellite Observations. Sensors. 2020; 20: 6881. https://doi.org/10.3390/s20236881 PMID: 33271976

30. Pitarch J, Volpe G, Colella S, Krasemann H, Santoleri R. Remote sensing of chlorophyll in the Baltic Sea at basin scale from 1997 to 2012 using merged multi-sensor data. Ocean Sci. 2016; 12: 379–389.

31. Lavigne H, Van der Zande D, Ruddick K, Dos Santos JC, Gohin F, Brotas V, et al. Quality-control tests for OC4, OC5 and NIR-red satellite chlorophyll-a algorithms applied to coastal waters. Remote Sens Environ. 2021; 255: 112237.

32. R Core Team. R: A Language and Environment for Statistical Computing. R Foundation for Statistical Computing. Vienna, Austria: R Foundation for Statistical Computing; 2020. Available: http://www.r-project.org/

33. Dowle M, Srinivasan A, Gorecki J, Chirico M, Stetsenko P, Short T, et al. Package 'data. table.' Ext 'data Frame. 2019.

34. Hijmans RJ, Phillips S, Leathwick J, Elith J, Hijmans MRJ. Package 'dismo.' Circles. 2017; 9: 1–68.

35. Pebesma EJ. Simple features for R: Standardized support for spatial vector data. R J. 2018; 10: 439.

36. Ridgeway G, Ridgeway MG. The gbm package. R Found Stat Comput Vienna Austria. 2004;5.

37. Bronaugh D, Werner A, Bronaugh MD. Package 'zyp.' CRAN Repos. 2009.

38. Grolemund G, Wickham H. Dates and times made easy with lubridate. J Stat Softw. 2011; 40: 1–25.

39. Wickham H. ggplot2: Elegant Graphics for Data Analysis. Springer-Verlag New York; 2009. Available: http://ggplot2.org

40. Eleveld MA, Ruescas AB, Hommersom A, Moore TS, Peters SWM, Brockmann C. An optical classification tool for global lake waters. Remote Sens. 2017;9. https://doi.org/10.3390/rs9050420

41. Messager ML, Lehner B, Grill G, Nedeva I, Schmitt O. Estimating the volume and age of water stored in global lakes using a geo-statistical approach. Nat Commun. 2016;7. https://doi.org/10.1038/ncomms13603 PMID: 27976671

42. Lehmann MK, Schütt EM, Hieronymi M, Dare J, Krasemann H. Analysis of recurring patchiness in satellite-derived chlorophyll a to aid the selection of representative sites for lake water quality monitoring. Int J Appl Earth Obs Geoinformation. 2021; 104: 102547. https://doi.org/10.1016/j.jag.2021.102547

43. Elith J, Leathwick J, Hastie T. A working guide to boosted regression trees. J Anim Ecol. 2008; 77: 802–813. https://doi.org/10.1111/j.1365-2656.2008.01390.x PMID: 18397250

44. Cohen AS, Gergurich EL, Kraemer BM, McGlue MM, McIntyre PB, Russell JM, et al. Climate warming reduces fish production and benthic habitat in Lake Tanganyika, one of the most biodiverse freshwater ecosystems. Proc Natl Acad Sci. 2016; 113: 9563–9568. https://doi.org/10.1073/pnas.1603237113 PMID: 27503877

45. Rugema E, Darchambeau F, Sarmento H, Stoyneva-Gärtner M, Leitao M, Thiery W, et al. Long-term change of phytoplankton in Lake Kivu: The rise of the greens. Freshw Biol. 2019; 64: 1940–1955. https://doi.org/10.1111/fwb.13383

46. Michalak AM, Anderson EJ, Beletsky D, Boland S, Bosch NS, Bridgeman TB, et al. Record-setting algal bloom in Lake Erie caused by agricultural and meteorological trends consistent with expected future conditions. Proc Natl Acad Sci. 2013; 110: 6448–6452. https://doi.org/10.1073/pnas.1216006110 PMID: 23576718

47. Rukhovets LA, Petrova NA, Menshutkin VV, Astrakhantsev GP, Minina TR, Poloskov VN, et al. Studying the response of Lake Ladoga ecosystem to a decrease in phosphorus load. Water Resour. 2011; 38: 806–817.

48. Kuhn C, Butman D. Declining greenness in Arctic-boreal lakes. Proc Natl Acad Sci. 2021; 118: e2021219118. https://doi.org/10.1073/pnas.2021219118 PMID: 33876758

49. Sommer U, Lewandowska A. Climate change and the phytoplankton spring bloom: warming and overwintering zooplankton have similar effects on phytoplankton. Glob Change Biol. 2011; 17: 154–162. https://doi.org/10.1111/j.1365-2486.2010.02182.x

50. O'Connor MIM, Piehler MFM, Leech DMD, Anton A, Bruno JF. Warming and resource availability shift food web structure and metabolism. PLoS Biol. 2009; 7: e1000178. https://doi.org/10.1371/journal.pbio.1000178 PMID: 19707271

51. Kraemer BM, Anneville O, Chandra S, Dix M, Kuusisto E, Livingstone DMDM, et al. Morphometry and average temperature affect lake stratification responses to climate change. Geophys Res Lett. 2015; 42: 4981–4988. https://doi.org/10.1002/2015GL064097

52. Richardson DC, Melles SJ, Pilla RM, Hetherington AL, Knoll LB, Williamson CE, et al. Transparency, geomorphology and mixing regime explain variability in trends in lake temperature and stratification across Northeastern North America (1975–2014). Water Switz. 2017; 9. https://doi.org/10.3390/w9060442

53. Winder M, Sommer U. Phytoplankton response to a changing climate. Hydrobiologia. 2012; 698: 5–16.

54. Multi-decadal improvement in US Lake water clarity—IOPscience. [cited 12 May 2021]. Available: https://iopscience.iop.org/article/10.1088/1748-9326/abf002/meta

55. Wilkinson G, Walter JA, Buelo C, Pace M. No evidence of widespread algal bloom intensification in hundreds of lakes. AGU; 2020. Available: https://agu.confex.com/agu/fm20/meetingapp.cgi/Paper/675321

56. Modabberi A, Noori R, Madani K, Ehsani AH, Mehr AD, Hooshyaripor F, et al. Caspian Sea is eutrophying: the alarming message of satellite data. Environ Res Lett. 2020; 15: 124047.

57. Stow CA, Dyble J, Kashian DR, Johengen TH, Winslow KP, Peacor SD, et al. Phosphorus targets and eutrophication objectives in Saginaw Bay: A 35year assessment. J Gt Lakes Res. 2014; 40: 4–10. https://doi.org/10.1016/j.jglr.2013.10.003

58. Archundia D, Duwig C, Spadini L, Uzu G, Guédron S, Morel MC, et al. How uncontrolled urban expansion increases the contamination of the titicaca lake basin (El Alto, La Paz, Bolivia). Water Air Soil Pollut. 2017; 228: 44.

59. Ignatieva NV. Distribution and release of sedimentary phosphorus in Lake Ladoga. Hydrobiologia. 1996; 322: 129–136. https://doi.org/10.1007/BF00031817

60. Woolway RI, Sharma S, Weyhenmeyer GA, Debolskiy A, Golub M, Mercado-Bettín D, et al. Phenological shifts in lake stratification under climate change. Nat Commun. 2021; 12: 2318. https://doi.org/10.1038/s41467-021-22657-4 PMID: 33875656

61. Feng L, Dai Y, Hou X, Xu Y, Liu J, Zheng C. Concerns about phytoplankton bloom trends in global lakes. Nature. 2021; 590: E35–E47. https://doi.org/10.1038/s41586-021-03254-3 PMID: 33597755

62. Palmer SCJ, Kutser T, Hunter PD. Remote sensing of inland waters: Challenges, progress and future directions. Remote Sens Environ. 2015; 157: 1–8. https://doi.org/10.1016/j.rse.2014.09.021

63. Matthews MW. A current review of empirical procedures of remote sensing in inland and near-coastal transitional waters. Int J Remote Sens. 2011; 32: 6855–6899.

64. De Senerpont Domis LN, Elser JJ, Gsell AS, Huszar VLM, Ibelings BW, Jeppesen E, et al. Plankton dynamics under different climatic conditions in space and time. Freshw Biol. 2013; 58: 463–482. https://doi.org/10.1111/fwb.12053